Lipid and Peptide Dynamics in Membranes upon Insertion of *n*-alkyl-β-D-Glucopyranosides

Matthias Meier[‡] and Joachim Seelig[†*]
[†]Department of Biophysical Chemistry, Biozentrum, University of Basel, Basel, Switzerland; and [‡]Department of Bioengineering, Stanford University, Stanford, California

ABSTRACT The effect of nonionic detergents of the *n*-alkyl-β-D-glucopyranoside class on the ordering of lipid bilayers and the dynamics of membrane-embedded peptides were investigated with ^{2}H- and ^{31}P-NMR. 1,2-dipalmitoyl-*sn*-glycero-3-phosphocholine was selectively deuterated at methylene segments C-2, C-7, and C-16 of the two fatty acyl chains. Two *trans*-membrane helices, WALP-19 and glycophorin A_{71-98}, were synthesized with Ala-d_3 in the central region of the α-helix. *n*-Alkyl-β-D-glucopyranosides with alkyl chains with 6, 7, 8, and 10 carbon atoms were added at increasing concentrations to the lipid membrane. The bilayer structure is retained up to a detergent/lipid molar ratio of 1:1. The insertion of the detergents leads to a selective disordering of the lipids. The headgroup region remains largely unaffected; the fatty acyl chain segments parallel to the detergent alkyl chain are only modestly disordered (10–20%), whereas lipid segments beyond the methyl terminus of the detergent show a decrease of up to 50%. The change in the bilayer order profile corresponds to an increase in bilayer entropy. Insertion of detergents into the lipid bilayers is completely entropy-driven. The entropy change accompanying lipid disorder is equivalent in magnitude to the hydrophobic effect. Ala-d_3 deuterated WALP-19 and $GlycA_{71-97}$ were incorporated into bilayers of 1,2-dimyristoyl-*sn*-glycero-3-phosphocholine at a peptide/lipid molar ratio of 1:100 and measured above the 1,2-dimyristoyl-*sn*-glycero-3-phosphocholine gel/liquid-crystal phase transition. Well-resolved ^{2}H-NMR quadrupole splittings were observed for the two *trans*-membrane helices, revealing a rapid rotation of the CD_3 methyl rotor superimposed on an additional rotation of the whole peptide around the bilayer normal. The presence of detergent fluidizes the membrane and produces magnetic alignment of bilayer domains but does not produce essential changes in the peptide conformation or dynamics.

INTRODUCTION

The solubilization of biological membranes by detergents, as well as the formation of membranes from micellar mixtures of detergents and lipids, has found wide application in membrane research. The most prominent example is the reconstitution of membrane proteins in functional form (1) or the preparation of lipid vesicles in defined form and composition (2). Very often, membrane solubilization protocols require mixtures of detergents rather than a single detergent (3,4). The optimization of the detergent mixture to either solubilize lipid membranes or purify membrane proteins in their native state is empirical and can be time-consuming. For a more rational approach, a quantitative understanding of the interaction of different detergent molecules with the lipid membrane and membrane protein is necessary.

Partitioning of detergents into lipid membranes and micelle formation are two energetically closely related processes, since both minimize unfavorable interactions of the detergent with water (5–10). Detergents can be categorized on the basis of their thermodynamic parameters, i.e., their partitioning coefficient (K_p) into lipid membranes and their critical micelle concentration (CMC). Strong detergents can be defined by $K_p \times CMC < 1$, weak detergents by $K_p \times CMC > 1$ (10). Thermodynamic comparison of a set of neutral detergents revealed that for a given hydrocarbon chain, strong detergents have a larger and more polar headgroup than weak detergents. Nevertheless, the classification of detergents on the basis of thermodynamic data alone is insufficient, and additional dynamic and structural information is needed to predict the specific interaction of detergents with lipid membranes. Membrane properties such as the packing density (11,12), the lipid chain order (13–16), the lateral mobility of lipids and proteins, or the curvature stress (17) are dependent on the specific chemical nature of the detergent and the average shape it adopts in a membrane environment.

The physical properties of the membrane lipids are important for the activity of membrane proteins, since the membrane perturbations induced by detergents can lead to changes in structure and function of the embedded proteins (18). Only the combined analysis of structural, dynamic, and thermodynamic parameters of the membrane solubilization process can lead to an understanding of detergent molecules and their impact on membrane proteins.

Here, we focus on the dynamic and structural changes of lipid membranes upon incorporation of nonionic *n*-alkyl-β-D-glucopyranosides of various chain lengths. These detergents have found widespread application in biological assays due to their nondenaturating effect on membrane proteins (19). *n*-Alkyl-β-D-glucopyranosides are known to act as lipid analogs and can be included in membranes at molar ratios >1 without membrane solubilization (10). Using solid-state ^{2}H- and ^{31}P-NMR spectroscopy, we monitored

Submitted September 14, 2009, and accepted for publication December 8, 2009.

*Correspondence: joachim.seelig@unibas.ch

Editor: Thomas J. McIntosh.

0006-3495/10/04/1529/10 $2.00

doi: 10.1016/j.bpj.2009.12.4286

the structural and dynamical changes of a model membrane composed of 1,2-dipalmitoyl-*sn*-glycero-3-phosphatidylcholine (DPPC) to which increasing amounts of detergent were added. The quadrupole splitting of selectively deuterated DPPC molecules in these lipid/detergent mixtures served as a quantitative marker of the membrane-disordering potential of the detergent, providing a detailed picture of the perturbation with a segment-to-segment resolution. In addition, we studied the dynamic and structural changes sensed by two membrane-bound peptides as *n*-alkyl-β-D-glucopyranosides were added to the membrane. We investigated two *trans*-membrane helices, the model peptide WALP-19 and the membrane-spanning domain of glycophorin A, both embedded in a membrane composed of 1,2-dimyristoyl-*sn*-glycero-3-phosphocholine (DMPC). The peptides were labeled with a methyl-deuterated alanine (Ala-d_3). The changes of the deuterium quadrupole splitting of the Ala-d_3 were exploited to detect structural and motional changes of the peptide within the peptide DMPC/*n*-alkyl-β-D-glucopyranosides mixtures. The addition of detergents produces significant changes in the order profile of the hydrocarbon chains. In contrast, the orientation and conformation of the membrane-spanning peptides is affected not at all or only a little.

MATERIALS AND METHODS

Detergent properties

Nonionic *n*-alkyl-β-D-glucopyranosides with chain lengths of 6, 7, 8, and 10 carbon atoms (denoted C-6, C-7, C-8, and C-10, respectively) were added to lipid membranes dispersed in buffer. The detergents were obtained from Fluka (Buchs, Switzerland) at the highest purity grade available. The CMC decreases with chain length and is 255 mM for C-6, 79 mM for C-7, 23 mM for C-8, and 2.2 mM for C-10 (10,20,21). The tendency to partition into a lipid membrane increases in the same order, i.e., the binding affinity increases with the length of the alkyl chain. Using a partition equilibrium of the form

$$X_b = c_{D,b}/c_L^0 = K_p c_{D,eq}, \quad (1)$$

where X_b is the molar amount of incorporated detergent per mol lipid, $c_{D,b}$ is the concentration of membrane-bound detergent, $c_{D,eq}$ is the equilibrium concentration of detergent, and c_L^0 is the total lipid concentration, the partition coefficients are $K_p = 8\ M^{-1}$, 40 M^{-1}, 120 M^{-1}, and 1600 M^{-1} for C-6, C-7, C-8, and C-10, respectively, as determined by isothermal titration calorimetry with bilayer vesicles composed of 1-palmitoyl-2-oleoyl-*sn*-glycero-3-phosphocholine (POPC) (see Table 2).

Preparation of lipid samples

The influence of detergents on membrane properties was investigated with bilayers composed of DPPC selectively deuterated at carbon atoms C-2, C-7, or C-16 of both palmitic acyl chains (22). A defined amount of deuterated lipid was transferred into an NMR sample tube (typically 5–8 mg of lipid) and mixed with nondeuterated DPPC (Avanti Lipids, Alabaster, AL) at a 1:4 molar ratio. Deuterium-depleted water was added (water/lipid ratio of 2:1, w/w) and the samples were extensively vortexed at room temperature with several freeze-thaw cycles in between, leading to multilamellar dispersions. Next, the *n*-alkyl-β-D-glucopyranoside was added in dry form. The sample was again extensively vortexed and several freeze-thaw cycles were performed. The amount of bound detergent, X_b, was calculated using the known partition coefficients, K_p, of the *n*-alkyl-β-D-glucopyranoside and rewriting Eq. 1 as

$$X_b = \frac{c_D^{total}}{c_L^0\left(1/K_p + 1\right)}, \quad (2)$$

where c_D^{total} is the total concentration of the added *n*-alkyl-β-D-glucopyranoside.

Peptide sample preparation

The WALP-19 peptide and the membrane-spanning helix of glycophorin A (GpA) were synthesized using standard *N*-(9-fluorenyl)methoxycarbonyl chemistry on a peptide synthesizer (433A, Applied Biosystems, Foster City, CA). Details of the peptide synthesis have been described previously (23,24). The amino acid sequences of the peptides were WALP-19 = NH_2-GWW$(LA)_6$LWWA-NH_2 and GpA fragment = NH_2-$_{71}$KKITL-IIFGV-MAGVI-GTILL-ISTGI-KK$_{98}$-COO^-. For a higher yield in the peptide synthesis, the natural GpA sequence was altered by omitting Pro^{72} and substituting Glu^{71}, Glu^{73}, Arg^{97}, and Arg^{98} with Lys residues. These amino acid substitutions have been shown to retain the GpA structure (25). Using Ala-CD_3, deuterium labels were inserted at position Ala^5 of WALP-19 and Ala^{82} of GpA. The crude peptides were purified by reverse-phase high-performance liquid chromatography. High-performance liquid chromatography and mass spectrometry revealed a purity of >91% for both peptides. The lyophilized peptides were dissolved in 2,2,2-trifluoroethanol (TFE) before use. A defined amount of peptide dissolved in TFE (usually 6 mg) was codissolved with DMPC in TFE to achieve a peptide/lipid molar ratio of 1:100. Solvent was removed and the mixture was dried overnight under high vacuum. Deuterium-depleted water was added to the mixture to yield a final water/lipid ratio of 2:1 (w/w). The samples were extensively vortexed at room temperature with several freeze-thaw cycles in between. The homogeneous peptide/lipid suspension was transferred to an NMR sample tube. Gradual increase of the detergent concentration was achieved by adding detergent in dry form.

NMR measurement

All ^{2}H- and ^{31}P-NMR experiments were performed on an Avance 400 MHz spectrometer (Bruker, Billerica, MA). DPPC-containing bilayers were measured at 45°C and DMPC-peptide-detergent samples at 30°C. These temperatures were well above the respective gel-to-liquid-crystal phase transition temperatures of $T_c = 41°$ for DPPC and $T_c = 23°C$ for DMPC. ^{2}H-NMR spectra were recorded at 61.4 MHz with the quadrupole echo technique. ^{31}P-NMR spectra were recorded at 161 MHz using a Hahn echo with broadband proton decoupling (WALTZ-16) and a recycle delay of 6 s. The phosphorus 31 chemical shielding anisotropy, $\Delta\sigma$, was measured in powder-type spectra as full width at 10% maximum intensity. The observed deuterium quadrupole splitting, $\Delta\nu_Q$,can be translated into the order parameter of the C-D bond vector according to

$$\Delta\nu_Q = (3/4)\left(\frac{e^2qQ}{h}\right)S_{CD}, \quad (3)$$

where $e^2qQ/h = 168$ kHz.

RESULTS

Membrane order profiles modified by *n*-alkyl-β-D-glucopyranosides: the effect of chain length

Deuterium NMR studies were undertaken to elucidate the structural and dynamic changes of lipid bilayers induced by the uptake of *n*-alkyl-β-D-glucopyranosides with alkyl

chain lengths of $n = 6$, 7, 8, and 10 carbons. Multilamellar bilayer dispersions were prepared from DPPC selectively deuterated at carbon atoms C-2, C-7, and C-16 of both palmitic acyl chains (22), and the variation of the quadrupole splitting upon incorporation of detergent was recorded. A decrease in molecular order of the lipid chain will decrease the quadrupole splitting.

Fig. 1 shows representative deuterium NMR spectra of C-7-labeled DPPC bilayers at 45°C with *n*-heptyl-β-D-glucopyranoside added at increasing concentrations. The line shape of the spectra is typical for liquid-crystalline bilayer domains oriented randomly with respect to the external magnetic field (powder-type spectra). The quadrupole splitting of the C-7 segment is 27.7 kHz at 45°C. At this chain segment, the *sn*-1 and *sn*-2 chains are motionally identical. Upon addition of *n*-heptyl-β-D-glucopyranoside, the quadrupole splitting decreases linearly with the mole fraction of detergent, X_b (Fig. 1) and the deuterium order parameter, S_{CD} (Fig. 2, *middle*). At the highest mole fraction measured ($X_b = 0.88$ mol/mole) the quadrupole splitting is reduced to 17.4 kHz. Extrapolated to 1 mol detergent, this corresponds to a reduction of ~42% referred to the quadrupole splitting of the detergent-free bilayer. An even larger reduction is observed for the incorporation of *n*-hexyl-β-D-glucopyranoside, a detergent with a shorter chain length. The opposite effect, i.e., less disorder, is caused by detergents with longer alkyl chains.

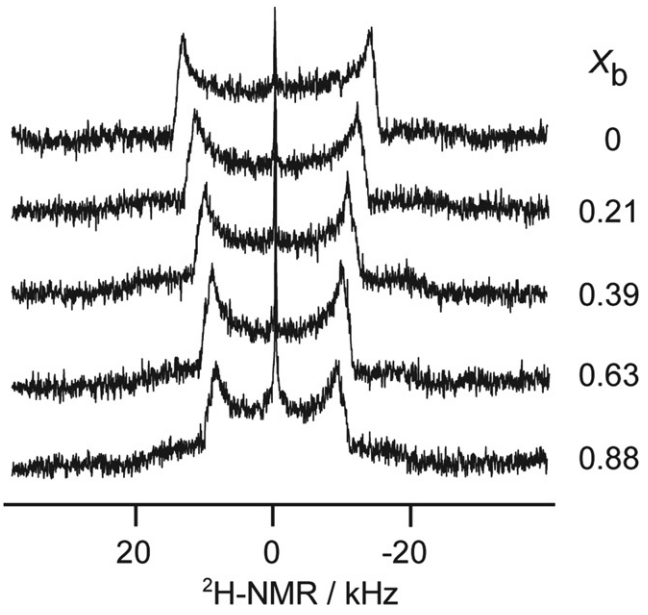

FIGURE 1 ^{2}H-NMR spectra of multilamellar dispersions of DPPC bilayers with *n*-heptyl-β-D-glucopyranoside. The DPPC molecule was selectively deuterated at the C-7 methylene segments of both palmitic acyl chains. X_b is the molar bound detergent/lipid ratio. The quadrupole splitting, defined by the separation of the two most intense peaks in the spectrum, decreases with the amount of incorporated detergent. Measurements were made at 45°C. The water/lipid ratio was 2:1.

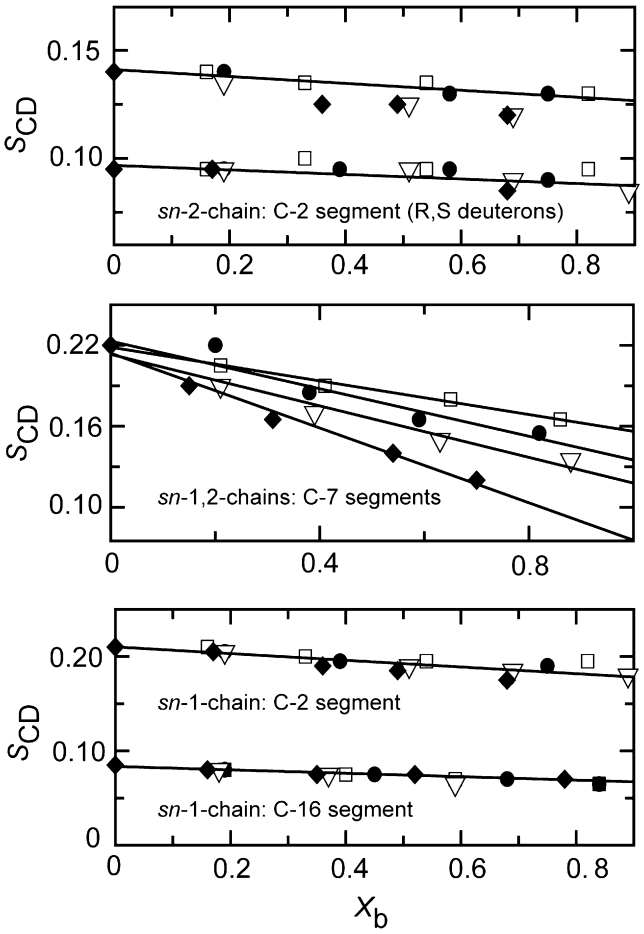

FIGURE 2 Variation of the order parameter, S_{CD}, for different bilayer segments as a function of the bound detergent-to-lipid ratio, X_b. The detergents are *n*-hexyl- (◆), *n*-heptyl- (▽), *n*-octyl- (●), and *n*-decyl-β-D-glucopyranoside (□).Solid lines represent the linear regression analysis.

Deuterium NMR spectra were also recorded for DPPC deuterium-labeled at the C-2 or the C-16 segment. For C-16 DPPC, only a single quadrupole splitting was observed for both fatty acyl chains. In contrast, the deuterium NMR spectrum of C-2 DPPC gives rise to three or four quadrupole splittings, respectively (Fig. 3). In the absence of detergents, the C-2 segment of the *sn*-1 chain displays a single quadrupole splitting with $\Delta\nu_Q = 26.8$ kHz, which is similar to the C-7 splitting. In contrast, the C-2 methylene group of the *sn*-2 chain shows two distinctly different quadrupole splittings with $\Delta\nu_Q = 17.9$ kHz and 11.8 kHz, as the two deuterons have different average orientations (26). The *sn*-1 chain is perpendicular to the membrane surface at all segments (27,28). The *sn*-2 chain, on the other hand, starts out parallel to the membrane surface and is bent by 90° after the C-2 segment. The orientation of the C-2 segment is thus quite different from those of all other alkyl carbon segments. In addition, the flexibility of this segment is rather restricted, so that the orientation of the two C-D bond vectors is not motionally averaged. The two factors together explain 1),

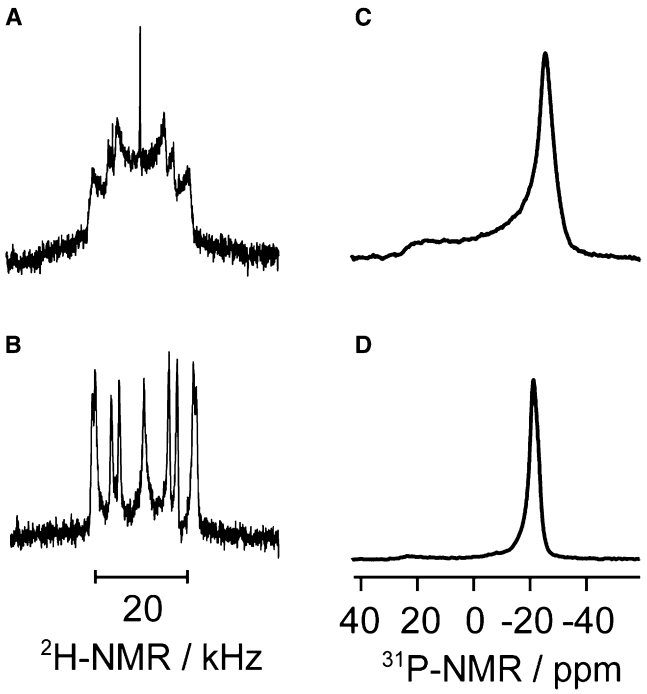

FIGURE 3 ^{2}H- and ^{31}P-NMR spectra of DPPC multilamellar dispersions deuterated at the C-2 segment of both palmitic acyl chains. The DPPC membrane contains *n*-hexyl-β-D-glucopyranoside at a molar detergent/lipid ratio of $X_b = 0.8$. (*A* and *C*) ^{2}H-NMR (*A*) and ^{31}P-NMR (*C*) spectra recorded immediately after insertion of the sample into the spectrometer. The spectra in *A* and *C* correspond to random dispersions of bilayer microdomains. (*B* and *D*) The same sample was recorded 30 min later. The single ^{31}P-NMR line in *D* located at the low-field edge of the ^{31}P-powder type spectrum (*B*) (at −20 ppm) provides evidence for a homogeneous alignment of the bilayer (with the bilayer normal perpendicular to the static magnetic field, B_0). The magnetic alignment reduces the linewidth in the ^{2}H-NMR spectrum (*C*) and allows the observation of four quadrupole splittings corresponding to the four deuterons at the two C-2 segments.

the reduced quadrupole splittings compared to the *sn*-1 chain, and 2), the motional and conformational inequivalence of the two C-2 deuterons of the *sn*-2 palmitic acyl chain.

The spectra displayed in Fig. 3 refer to C-2-deuterated DPPC bilayers containing 0.8 mol *n*-hexyl-β-D-glucopyranoside/mol DPPC. These spectra were recorded immediately after insertion of the sample into the NMR spectrometer (Fig. 3, *A* and *C*) and 30 min later (Fig. 3, *B* and *D*). During this time interval, the bilayers become aligned in the magnetic field. In Fig. 3 *A*, the bilayer domains are distributed at random, and in Fig. 3 *B*, the domains are oriented homogeneously such that the bilayer normal is perpendicular to the magnetic field. This is most clearly documented by the phosphorus 31 NMR spectrum (Fig. 3 *D*), which gives rise to a sharp line at the position of the low-field edge of the powder-type spectrum seen in Fig. 3 *C*. A magnetic alignment of phospholipid bilayer in the NMR spectrometer was first observed and analyzed for phospholipid mixtures composed of anionic and neutral lipids (29). In this study, the addition of nonionic *n*-hexyl-β-D-glucopyranoside also induces sufficient mobility of the microdomains to allow bilayer alignment. No alignment was observed with detergents with longer chain length. However, magnetic orientation was observed for the nonionic detergent octaethyleneglycol mono-*n*-dodecylether ($C_{12}E_6$) when incorporated into different phospholipid bilayers at a phospholipid/detergent molar ratio of 2:1 (15).

The magnetic alignment leads to sharper resonance lines. Fig. 3 *B* then reveals a small motional inequivalence of the two deuterons of the *sn*-1 chain with quadrupole splittings of 22.6 kHz and 21.1 kHz. The quadrupole splittings of the *sn*-2 chain in the same sample are 15.1 kHz and 10.9 kHz. To our knowledge, the spectrum shown in Fig. 3 *B* is the first observation of an inequivalence of all four C-2 deuterons.

Fig. 2 provides a quantitative comparison of all detergents and DPPC segments investigated. The order parameter, S_{CD}, is plotted as a function of bound detergent, measured by its mole fraction, X_b. The figure demonstrates that the four detergents produce virtually identical effects at the C-2 and C-16 segments. The order parameters decrease by only ~10% upon addition of 1 mol detergent, independent of the length of the alkyl chain. For the C-7 segment, a different result is obtained. Here, the order parameter is clearly dependent on the length of the alkyl chain and decreases most distinctly upon insertion of *n*-hexyl-β-D-glucopyranoside. The perturbation is less pronounced for the longer chains; however, even for the C-10 detergent the reduction of the order parameter is remarkably larger than observed either at the C-2 or the C-16 segment. Fig. 2 then provides evidence for two different effects: 1), a general disordering at all segments by ~10%; and 2), a specific disordering near the end of the inserted hydrocarbon chain of the detergent of up to 50%.

A sufficiently high concentration of *n*-alkyl-β-D-glucopyranosides will disrupt the bilayer structure. Using phosphorus-31 NMR, we determined the critical X_b values for the disruption of DPPC bilayers to be $X_b^{crit} = 1.4 \pm 0.1$, 1.5 ± 0.1, 1.5 ± 0.1, and 1.7 ± 0.1 for alkyl chain lengths of $n = 6$, 7, 8, and 10, respectively. Incorporation of long-chain detergents is obviously better tolerated than that of short-chain detergents.

Detergent partitioning and solubilization of lipid membranes containing *trans*-membrane helices

As *n*-alkyl-β-D-glucopyranosides perturb the lipid membrane, we were interested in knowing whether this perturbation also extends to membrane proteins and may influence their solubilization. We synthesized two well-studied *trans*-membrane peptides, that is, 1), the model peptide WALP-19 (30,31) and 2), the membrane-spanning part of GpA (32). Both peptides form *trans*-membrane helices when incorporated into bilayers of DMPC, with WALP-19 being monomeric and GpA homodimeric. We introduced deuterated

alanine residues (Ala-d_3) in both peptides to monitor their conformation, mobility, and orientation. The deuterium quadrupole splitting of the deuterons attached to the methyl group is dependent on the mobility and orientation of the C_α-C_β bond axis of the alanine residue (30,31,33).

The quadrupole splitting of the freely rotating methyl rotor (-CD_3) can be calculated as $|\Delta\nu_Q| = 84$ kHz assuming tetrahedral bond angles and an orientation of the rotor axis (C_α-C_β bond vector) exactly parallel to the static magnetic field. For a random distribution of rotor axes (powder-type spectrum), the separation of the two most intense peaks in the spectrum is 42 kHz. Additional motions of the methyl rotor will further reduce the quadrupole splitting.

In the studies described here, the deuterated alanine is part of a *trans*-membrane α-helix. The α-helix constitutes an additional element of rotational averaging, either by a fast rotation around the helix axis itself or by a rotation of a tilted α-helix around the bilayer normal. Based on crystal structures, the C_α-C_β axis of the -CD_3 rotor makes an angle of ~56.2° with the helix axis (30), which is close to the so-called magic angle of 57.4°. For an α-helix oriented exactly parallel to the bilayer normal, the quadrupole splitting of the powder-type spectrum is thus reduced from 42 kHz to 1.5 kHz. Small changes in the α-helix orientation or in the α-helix conformation would induce relatively large changes in the quadrupole splitting. For example, if the C_α-C_β rotation axis is inclined at $\theta = 60°$, a quadrupole splitting of $\Delta\nu_Q = 5.2$ kHz would be observed.

Fig. 4 shows ^{2}H-NMR spectra of Ala^5-labeled WALP-19 in DMPC bilayers (peptide/DMPC molar ratio 1:100) at

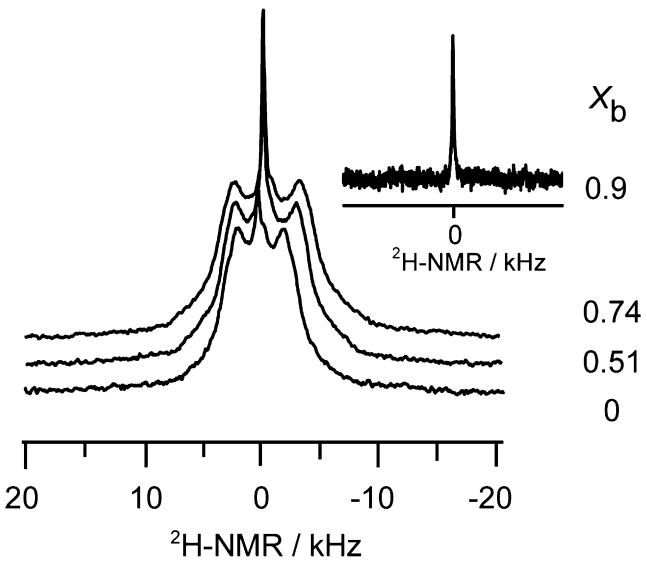

FIGURE 4 Deuterium NMR spectra of Ala-d_3-labeled WALP-19 incorporated into mixtures of *n*-hexyl-β-D-glucopyranoside with DMPC. X_b is the molar detergent/lipid ratio. The molar peptide/lipid ratio is 1:100 in all spectra.

increasing concentrations of *n*-hexyl-β-D-glucopyranoside. At 30°C, the measured quadrupole splitting is 4.1 kHz, corresponding to 8.2 kHz in an aligned spectrum. This is somewhat larger than a previous value of 6.6 kHz observed for the same peptide in aligned DMPC bilayers measured at 40°C (30). Increasing concentrations of detergent lead to a small increase in the quadrupole splitting by ~1.8 kHz per mole detergent. The WALP-19/DMPC/detergent bilayer is stable up to $X_b^{crit} = 0.9$, i.e., almost up to a 1:1 detergent/lipid molar ratio. Depending on the structure of the *trans*-membrane peptide and its lipid environment, much larger quadrupole splittings have been observed for Ala-CD_3 (33). The small quadrupole splitting recorded here for WALP-19 provides evidence of a sufficiently fast rotation of the peptide around its α-helix axis to further average the static quadrupole coupling.

The analogous experiment was performed with WALP-19 and *n*-octyl-β-D-glucopyranoside. We found the same increase in the quadrupole splitting per mole of detergent. The stability of the WALP-19/DMPC/detergent bilayer increased to $X_b^{crit} = 1.4$.

As a second example, for detergent/lipid/peptide interactions, we investigated the membrane-spanning fragment of GpA, a peptide of 27 amino acids. Dimerization of two GpA helices in a lipid membrane environment is dependent on the seven-residue motif ^{75}LIxxG-VxxGV-xxT^{88}. These amino acids are located on one side of the α-helix axis, forming the contact interface between two GpA helices (32,34). We labeled the peptide at the Ala^{83} residue (numbering taken from the full-length protein), which is located on the opposite side of the contact interface of a GpA dimer. The deuterons of Ala^{83} are thus not involved in the contact of the two GpA molecules and can freely rotate. The α-helix axis of GpA is tilted by ~30 ° with respect to the bilayer normal and it can be estimated that the -CD_3 group is located in the hydrophobic interior of the DMPC bilayer (32). It has been shown that incorporation of GpA in DMPC lipid bilayers produces only a small increase of acyl chain disorder of DMPC membranes (35).

Fig. 5 shows deuterium NMR spectra of Ala-d_3-labeled GpA in DMPC bilayers at a peptide/lipid molar ratio of 1:100 with various concentrations of *n*-hexyl- or *n*-octyl-β-D-glucopyranoside. In pure DMPC membranes and in DMPC bilayers with low detergent concentrations, a broad deuterium signal with a low signal/noise ratio was observed. The resolution and the signal/noise ratio increased, however, as the concentration of detergent in the DMPC membrane increased. Independent of the chain length of the detergents, the deuterium NMR spectra at high detergent concentration revealed two sets of deuterium quadrupole splittings with separations of 4–6 kHz and 16–20 kHz, indicating two different orientations of the -CD_3 rotor. The measured quadrupole splittings for WALP-19 and GpA in various lipid/detergent systems are summarized in Table 1.

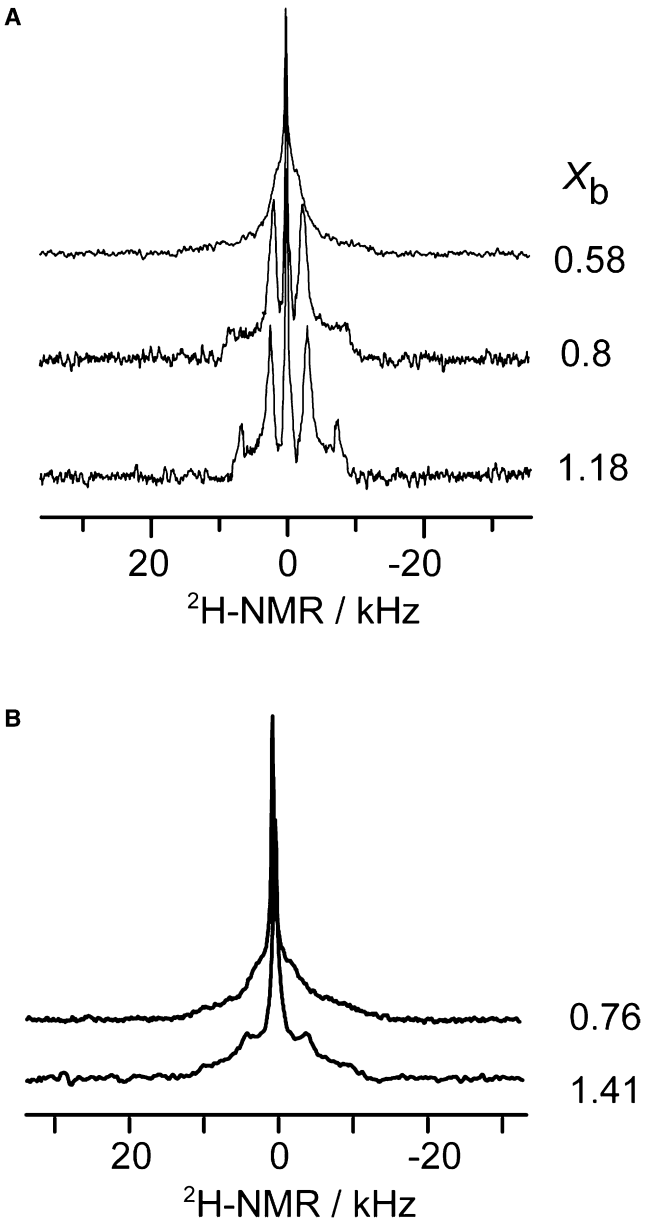

FIGURE 5 Deuterium NMR spectra of Ala-d_3-labeled GpA incorporated into mixtures of (*A*) *n*-hexyl- and (*B*) *n*-octyl-β-D-glucopyranoside with DMPC. The peptide/lipid ratio is 1:100 in all spectra. In the case of *n*-hexyl-β-D-glucopyranoside, the resolution of the ^{2}H-NMR spectra increases with increasing detergent concentration as the bilayer microdomains align in the magnetic field.

DISCUSSION

Detergent-induced distortion of the bilayer order profile

The insertion of *n*-alkyl-β-D-glucopyranosides induces considerable changes in the ordering of bilayer lipids. These become understandable by considering the surface area of the glucose moiety in relation to the cross-sectional area of its attached hydrocarbon chain. The surface area requirement

TABLE 1 Quadrupole splittings, $\Delta\nu_Q$, of WALP-19 and GpA *trans*-membrane helices in membranes with detergents

	WALP-19		Glycophorin A		
	X_b (mol/mol)	$\Delta\nu_Q$ (kHz)	X_b (mol/mol)	$\Delta\nu_Q$ (kHz)	$\Delta\nu_Q$ (kHz)
β-D-hexyl-glucopyranoside					
	0	4.2	0	3	~32
	0.51	5	0.058	4.7	23
	0.74	5.6	0.8	4.1	18.5
			1.18	5.9	14.1
β-D-octyl-glucopyranoside					
	0	4.1	0	3	~32
	0.3	4.8	0.76	4.9	~26
	0.72	5.6	1.41	7.5	21

of *n*-octyl-β-D-glucopyranoside at the air/water interface was determined previously by means of the Gibbs adsorption isotherm as $A_S = 51 \pm 3$ Å^2 (36). In parallel, using the phospholipid monolayer expansion method, the insertion area of *n*-octyl-β-D-glucopyranoside at the monolayer-bilayer equivalence pressure of 32 mN/m was found to be $A_I = 58 \pm 10$ Å^2 (36,37). By comparison with molecular models, it can be concluded that *n*-octyl-β-D-glucopyranoside penetrates between the phospholipids such that the glucose moiety lies flat between the phospholipid headgroups. However, the cross-sectional area of a hydrocarbon chain is only ~25 Å^2, and the insertion of the glucose residue between the phospholipid headgroups thus creates a void volume in the hydrophobic part of the membrane.

It is important to note that the sugar moiety does not affect the phospholipid headgroup conformation. This was demonstrated for a related bilayer system, POPC (36). ^{2}H- and ^{31}P-NMR showed that addition of *n*-octyl-β-D-glucopyranoside up to a molar ratio of $X_b = 1.3$ mol/mol left the POPC bilayer structure fully intact and produced almost no change in the orientation of the phosphocholine dipole or in the motion and conformation of the C-2 chain segments. A modest reduction (~18%) of the quadrupole splitting was found for the C-5 segment of POPC but a 30–50% reduction occurred for segments 9–12. Together with the data presented here, a characteristic response of the lipid bilayer toward *n*-alkyl-β-D-glucopyranosides can be deduced: 1), The phospholipid headgroup and the glycerol backbone regions are not changed by the insertion of the glucose moiety. Adsorption of additional water molecules, perhaps hydrogen-bonded to the hydroxyl groups of the sugar ring, must fill newly created void volume. 2), In the hydrophobic part of the bilayer, the molecular order of the lipid chains is modestly reduced for segments neighboring the inserted detergent chains. On the other hand, segments near the tail end of the detergent experience much larger distortions (30–50%) to compensate for the void space created near the -CH_3 terminus. For DMPC bilayers, the disordering effect is expected to be largest for the surfactant with the

shortest alkyl chain, as it creates the largest void volume (cf. Fig. 2, *C-7 segment*).

Thermodynamic aspects

The NMR data can be extended by considering the thermodynamic aspects accompanying detergent insertion. Table 2 summarizes the thermodynamic data for micelle formation of *n*-alkyl-β-D-glucopyranosides. Likewise, the table contains the binding constant, K_p, and the insertion enthalpy, ΔH^0_p, of the same detergents upon insertion into POPC bilayers. Micelle formation and membrane insertion are processes with similar free energies. A comparison of ΔG^0_{mic} to ΔG^0_p as a function of the alkyl chain length is given in Fig. 6 *A*. For both reactions, ΔG^0 depends linearly on the chain length with almost identical slopes of $\Delta G_{CH_2} = -0.7$ kcal/mol, which is the free energy of the insertion of a single CH_2 group. Extrapolation to $n = 0$ yields $\Delta G^0_{headgroup} = 3.35$ kcal/mol for the insertion of the glucose headgroup. The monolayer-bilayer equivalence pressure is about $\pi = 32$ mN/m (37) and the intercalation of a headgroup of area 0.58 nm^2 into the bilayer requires hence the molar energy $\Delta G^0_{hg} = A_I \pi N_A = 2.67$ kcal/mol, which is in broad agreement with the extrapolated value.

The enthalpies of micelle formation and lipid partitioning are endothermic, small, and almost independent of temperature. The driving force for micelle formation and membrane insertion is thus the entropy in both cases. Fig. 6 *B* compares the entropy of micelle formation, ΔS^0_{mic}, with the entropy of detergent partitioning, ΔS^0_p, as a function of chain length, *n*. The two data sets are almost identical, and linear regression analysis yields

$$\Delta S^0_p(\text{cal/molK}) = 2.23n - 4.45.$$

The entropy gain of $\Delta S^0_{CH_2} = 2.23$ cal/molK/inserted CH_2 segment is usually ascribed to the hydrophobic effect. The molecular origin of the hydrophobic effect is a release of water molecules as the hydrated alkyl chain is accommodated between the equally hydrophobic fatty acyl chains of the lipids. However, the disordering of the lipid hydrocarbon chains is an additional entropy source of considerable magnitude (38). This effect has received little attention so far but becomes obvious from a comparison of the solid-to-fluid transition of simple hydrocarbons with the gel-to-liquid crystal transition of phospholipid bilayers. The melting of solid fatty acids or paraffins requires an incremental transition enthalpy of $\Delta H_{CH_2} = 1.0$ kcal/mol, and the corresponding transition entropy is $\Delta S_{CH_2} = 2.6$ cal/mol K (39–41). In contrast, the gel-to-liquid crystal transition of phospholipids with two saturated and linear hydrocarbon chains requires a smaller enthalpy of only $\Delta H_{CH_2} = 0.5$ kcal/mol and a smaller entropy, $\Delta S_{CH_2} = 1.3$–1.6 cal/mol K. Thus, there is a potential gain of $\Delta S_{CH_2} = 1.0$–1.3 cal/molK for a full melting of the hydrocarbon chains in the lipid bilayer.

Next, we correlate the entropy change with the change in order parameter, $P_2 = (3\langle\cos^2\Theta\rangle - 1)/2$, of the long molecular axis. In crystalline hydrocarbons, the -$(CH_2)_n$- chains are essentially in the all-*trans* conformation, $\langle\cos^2\Theta\rangle = 1$ (no fluctuation), and $P_2 = 1$. The melting of a solid paraffin chain with $P_2 = 1$ to an isotropic liquid paraffin with $P_2 = 0$ corresponds to a change in order parameter of $\Delta P_2 = 1$. Correspondingly, the phase transition of a lipid bilayer from the gel state with ordered all-*trans* fatty acyl chains and $P_2 \sim 1$ to a liquid-crystalline bilayer with $P_2 \sim 0.4$ entails $\Delta P_2 = 0.6$. Finally, nematic liquid crystals, which are essentially rigid rods, undergo a temperature-induced transition from a liquid-crystalline phase to an isotropic liquid. At the transition temperature, the order parameter of the liquid-crystal phase is $P_2 \sim 0.44$, and the approximate transition entropy

TABLE 2 Thermodynamic properties of *n*-alkyl-β-D-glucopyranosides

			Micelle formation				Membrane partitioning				
Chain length (*n*)	T* K	CMC† (mM)	ΔH^0_{mic}‡ kcal/mol	ΔG_{mic}¶ (kcal/mol)	ΔS_{mic}** (cal/molK)	Reference	K_P†† (M^{-1})	ΔH^0_P‡‡ (kcal/mol)	ΔG_P¶¶ (kcal/mol)	ΔS_P*** cal/molK	Reference
6		255	1.78625	−0.81	8.70		8‖	1.41‖	−1.23‖	8.85‖	
7		79	1.87	−1.50	11.30	49	40‖	1.35‖	−2.18‖	11.83‖	
8		23	1.73	−2.23	13.27	50	120	1.29	−2.82	13.81	(36)
8		23.5	1.87	−2.21	13.70	49					
8			1.53			51					
8	27	22.6	1.68	−2.24	13.14	52					
9		6.5	1.87	−2.97	16.25	49					
9	20	8	1.95	−2.85	16.10	52					
10		2.3	1.79	−3.58	18.03	51	1600	1.17	−4.35	18.54	(21)
10	20	2.29	1.49	−3.59	17.04	52					

*Temperature.
†Critical micelle concentration.
‡, ¶, **Enthalpy, free energy, and entropy of micelle formation.
††Detergent partition coefficient.
‡‡, ¶¶, ***Enthalpy, free energy, and entropy of detergent partitioning.
‖X. Li-Blatter and A. Seelig, unpublished measurement.

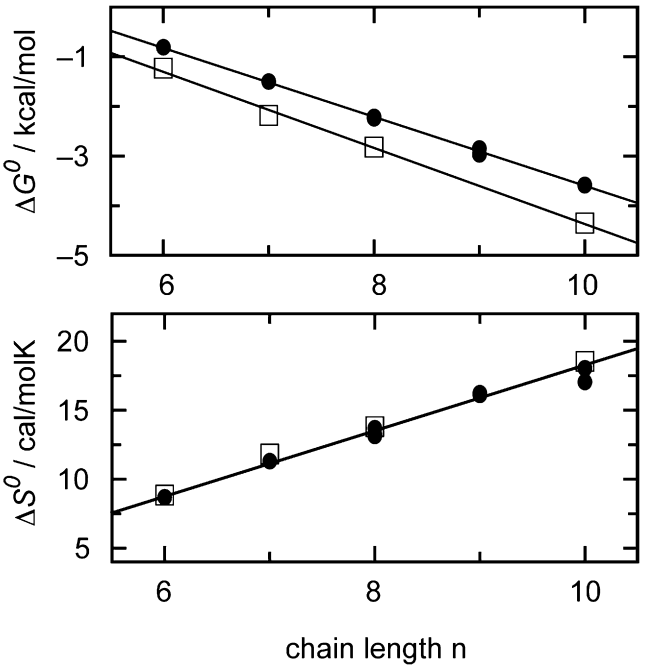

FIGURE 6 Thermodynamics of micelle formation of *n*-alkyl-β-D-glucopyranosides compared to membrane partitioning of the detergents into POPC bilayers. (*A*) Variation of the Gibbs free energies of micelle formation, ΔG^0_{mic} (•), and membrane partitioning, ΔG^0_p (□), as a function of *n*-alkyl chain length. (*B*) Comparison of the entropy of micelle formation, ΔS^0_{mic} (•) with membrane partitioning, ΔS^0_p (□).

associated with the transition to an isotropic liquid is 0.83 cal/molK for $\Delta P_2 = 0.44$ (42). Taken together, these data suggest a linear correlation between the change in entropy, ΔS_{CH_2}, and the change in the molecular order parameter of hydrocarbon chains according to

$$\Delta S_{CH_2}(\text{cal/molk}) \approx 2.6\Delta P_2 (R \sim 0.99).$$

Applied to the measured changes in the quadrupole splittings of DPPC bilayers described in Fig. 2, this result leads to the following conclusion. Taking the average of all hydrocarbon segments, the insertion of 1 mol detergent can change the quadrupole splitting by 20–25%, corresponding to a change in the order parameter of the long molecular axis by $\Delta P_2 = 2|\Delta S_{CD}| \approx 0.1$. For a phospholipid molecule with 30 CH_2/CH_3 segments, this would produce an entropy increase of 7.8 cal/molK. This is comparable, for example, to the entropy change of 8.9 cal/molK observed for the insertion of 1 mol hexyl-*n*-β-D-glucopyranoside into DPPC bilayers.

Protein dynamics in the presence of detergents

This study addresses the question of how the destabilization of the lipid matrix with detergent may affect the motion of the protein. For the rigid *trans*-membrane helix of WALP-19, the answer is simple: up to the highest detergent concentration employed, the deuterium quadrupole splitting increases only slightly. Even at conditions close to membrane micellization (at a *n*-hexyl-β-D-glucopyranoside-to-lipid ratio of 0.9 mol/mol) no change in the motion of WALP-19 is observed. This result is perhaps not unexpected. As mentioned above, the headgroup region of the phosphocholine lipid bilayer is stable and not modified by the insertion of the glucose ring. As the WALP-19 helix is extending with both ends into opposite headgroup regions, it is rigidly anchored and will not sense the disordering of the hydrocarbon chains in the hydrophobic part of the bilayer.

A somewhat different picture is obtained for the GpA fragment. GpA is a natural protein that forms homodimers in lipid bilayers (34). The phase behavior of the DMPC/GpA system has been investigated with perdeuterated DMPC (32,35). At low peptide concentrations (~1% molar concentration)—as also employed in this study—the ^{2}H-NMR data show virtually no change of the hydrocarbon chain ordering at temperatures above the gel-to-liquid crystal transition. This is in agreement with many other NMR observations, providing evidence for a fluidlike match between the outer surface of a membrane protein and the surrounding lipids (43–47).

Earlier deuterium NMR studies used perdeuterated valines in the *trans*-membrane sequence (24). The peptide was labeled at three different positions (val^{80}, val^{82}, and val^{84}), incorporated into DMPC bilayers at a 1:40 lipid/protein ratio and measured at 20°C and 60°C. The single C_α and C_β deuterons were not detected, indicating a very rigid peptide structure so that the quadrupole splittings are near the rigid limit of 126 kHz (nonoriented sample). The only observed intensity resulted from the methyl rotors. The measured quadrupole splittings were ~30 kHz and consistent with a model of only rapid -CD_3 rotation, with little motion of the C_α-C_β bond or additional rotation around the helix axis. No differences were found between the peptide dimer and monomer.

This study reveals a somewhat different picture. Superimposed on the fast CD_3 rotation of Ala^{82} are additional motions that further reduce the quadrupole splittings either to ~5 kHz at low detergent concentrations or to ~5 and ~20 kHz at higher detergent concentrations. It is rather unlikely that the observed changes are caused by a dissociation of the GpA dimer. The association equilibrium of the peptide was measured in a variety of detergents (above the respective micellar concentration) and the dissociation constants were all in the micromolar range (48). It can be expected that the dissociation constant is even lower in an orderly packed bilayer. On the other hand, the insertion of *n*-hexyl- or *n*-octyl-β-D-glucopyranoside into DMPC bilayers fluidizes the membrane, as is obvious from the reduced linewidth at high detergent concentration. In parallel, this could produce two different dimer populations or an asymmetric dimer molecule with two different average orientations of the methyl rotor. As mentioned above, a difference of $\leq 5^\circ$ would be sufficient to explain the differences in

the quadrupole splittings. Hence, minor variations in the structure of the GpA dimer are sufficient to explain the deuterium NMR spectra.

n-Alkyl-β-D-glucopyranosides are frequently used in purification steps in membrane proteins, as they leave the protein structure intact. The spectra shown here support this empirical finding, in that the *n*-alkyl-β-D-glucopyranosides induce only minor changes in the structure of the two membrane proteins investigated here.

CONCLUSIONS

The insertion of *n*-alkyl-β-D-glucopyranosides into lipid bilayers leads to specific changes in the bilayer order profile. Unexpectedly, perhaps, the intercalation of the glucose moiety between the phospholipid headgroups causes no or only small changes at the level of the phosphocholine dipole, the glycerol backbone, and the C-2 segments of the fatty acyl chains, even at a detergent/lipid ratio of 1:1, which is close to bilayer disruption. A different result is observed for the hydrophobic part of the bilayer. The ordering of the fatty acyl chains, as measured by the quadrupole splitting $\Delta\nu_Q$, is reduced by 10–20% for CH_2 segments neighboring the *n*-alkyl chain of the detergents. However, a reduction of up to 50% is seen for fatty acyl segments in the void volume behind the terminal methyl group of the detergent. *Trans*-membrane helices appear not to sense the disordering effect of the detergents employed in this study, as judged by the behavior of Ala-d_3 incorporated in the middle of the α-helix. Detergent addition fluidizes the membrane, sharpens the linewidth, and induces a magnetic alignment of the bilayer lipid, with and without protein. The partitioning of *n*-alkyl-β-D-glucopyranosides is exclusively entropy-driven. The change in the order parameter, P_2, can be correlated with the change in the entropy, ΔS. The increased disorder of the fatty acyl chain upon detergent insertion could almost completely account for the experimentally observed change in entropy.

This work was supported by the Swiss National Science Foundation (grant 3100-107793).

REFERENCES

1. Privé, G. G. 2007. Detergents for the stabilization and crystallization of membrane proteins. *Methods*. 41:388–397.
2. Ueno, M., C. Tanford, and J. A. Reynolds. 1984. Phospholipid vesicle formation using nonionic detergents with low monomer solubility. Kinetic factors determine vesicle size and permeability. *Biochemistry*. 23:3070–3076.
3. Grisshammer, R., J. F. White, …, J. Shiloach. 2005. Large-scale expression and purification of a G-protein-coupled receptor for structure determination—an overview. *J. Struct. Funct. Genomics*. 6:159–163.
4. Yeliseev, A. A., K. K. Wong, …, K. Gawrisch. 2005. Expression of human peripheral cannabinoid receptor for structural studies. *Protein Sci.* 14:2638–2653.
5. Lichtenberg, D., R. J. Robson, and E. A. Dennis. 1983. Solubilization of phospholipids by detergents. Structural and kinetic aspects. *Biochim. Biophys. Acta*. 737:285–304.
6. Jackson, M. L., C. F. Schmidt, …, A. D. Albert. 1982. Solubilization of phosphatidylcholine bilayers by octyl glucoside. *Biochemistry*. 21:4576–4582.
7. Almog, S., B. J. Litman, …, D. Lichtenberg. 1990. States of aggregation and phase transformations in mixtures of phosphatidylcholine and octyl glucoside. *Biochemistry*. 29:4582–4592.
8. Ollivon, M., O. Eidelman, …, A. Walter. 1988. Micelle-vesicle transition of egg phosphatidylcholine and octyl glucoside. *Biochemistry*. 27:1695–1703.
9. Lichtenberg, D. 1985. Characterization of the solubilization of lipid bilayers by surfactants. *Biochim. Biophys. Acta*. 821:470–478.
10. Heerklotz, H., and J. Seelig. 2000. Titration calorimetry of surfactant-membrane partitioning and membrane solubilization. *Biochim. Biophys. Acta*. 1508:69–85.
11. Aagaard, T. H., M. N. Kristensen, and P. Westh. 2006. Packing properties of 1-alkanols and alkanes in a phospholipid membrane. *Biophys. Chem.* 119:61–68.
12. Thurmond, R. L., D. Otten, …, K. Beyer. 1994. Structure and packing of phosphatidylcholines in lamellar and hexagonal liquid-crystalline mixtures with a nonionic detergen: a wide-line deuterium and phosphorus-31 NMR study. *J. Phys. Chem.* 98:972–983.
13. McIntosh, T. J., S. A. Simon, and R. C. MacDonald. 1980. The organization of *n*-alkanes in lipid bilayers. *Biochim. Biophys. Acta*. 597:445–463.
14. Westerman, P. W., J. M. Pope, …, D. W. Dubro. 1988. The interaction of *n*-alkanols with lipid bilayer membranes: a 2H-NMR study. *Biochim. Biophys. Acta*. 939:64–78.
15. Otten, D., L. Löbbecke, and K. Beyer. 1995. Stages of the bilayer-micelle transition in the system phosphatidylcholine-C12E8 as studied by deuterium- and phosphorous-NMR, light scattering, and calorimetry. *Biophys. J.* 68:584–597.
16. Otten, D., M. F. Brown, and K. Beyer. 2000. Softening of membrane bilayers by detergents elucidated by deuterium NMR spectroscopy. *J. Phys. Chem. B*. 104:12119–12129.
17. Ly, H. V., and M. L. Longo. 2004. The influence of short-chain alcohols on interfacial tension, mechanical properties, area/molecule, and permeability of fluid lipid bilayers. *Biophys. J.* 87:1013–1033.
18. Cantor, R. S. 1999. Solute modulation of conformational equilibria in intrinsic membrane proteins: apparent ''cooperativity'' without binding. *Biophys. J.* 77:2643–2647.
19. Stubbs, G. W., H. G. Smith, Jr., and B. J. Litman. 1976. Alkyl glucosides as effective solubilizing agents for bovine rhodopsin. A comparison with several commonly used detergents. *Biochim. Biophys. Acta*. 426:46–56.
20. Kobayashi, T., S. Adachi, and R. Matsuno. 1999. Synthesis of alkyl fucosides through β-blucosidase-catalyzed condensation of fucose and 1-alcohols. *Biotechnol. Lett.* 21:105–109.
21. Heerklotz, H., and J. Seelig. 2000. Correlation of membrane/water partition coefficients of detergents with the critical micelle concentration. *Biophys. J.* 78:2435–2440.
22. Seelig, A., and J. Seelig. 1974. The dynamic structure of fatty acyl chains in a phospholipid bilayer measured by deuterium magnetic resonance. *Biochemistry*. 13:4839–4845.
23. Greathouse, D. V., R. L. Goforth, …, J. A. Killian. 2001. Optimized aminolysis conditions for cleavage of N-protected hydrophobic peptides from solid-phase resins. *J. Pept. Res.* 57:519–527.
24. Liu, W., E. Crocker, …, S. O. Smith. 2003. Role of side-chain conformational entropy in transmembrane helix dimerization of glycophorin A. *Biophys. J.* 84:1263–1271.
25. Fang, C., A. Senes, …, R. M. Hochstrasser. 2006. Amide vibrations are delocalized across the hydrophobic interface of a transmembrane helix dimer. *Proc. Natl. Acad. Sci. USA*. 103:16740–16745.
26. Seelig, A., and J. Seelig. 1975. Bilayers of dipalmitoyl-3-*sn*-phosphatidylcholine. Conformational differences between the fatty acyl chains. *Biochim. Biophys. Acta*. 406:1–5.

27. Büldt, G., H. U. Gally, …, G. Zaccai. 1978. Neutron diffraction studies on selectively deuterated phospholipid bilayers. *Nature*. 271:182–184.

28. Büldt, G., H. U. Gally, …, G. Zaccai. 1979. Neutron diffraction studies on phosphatidylcholine model membranes. I. Head group conformation. *J. Mol. Biol.* 134:673–691.

29. Seelig, J., F. Borle, and T. A. Cross. 1985. Magnetic ordering of phospholipid membranes. *Biochim. Biophys. Acta.* 814:195–198.

30. van der Wel, P. C., E. Strandberg, …, R. E. Koeppe, 2nd. 2002. Geometry and intrinsic tilt of a tryptophan-anchored transmembrane α-helix determined by (2)H NMR. *Biophys. J.* 83:1479–1488.

31. Strandberg, E., S. Ozdirekcan, …, J. A. Killian. 2004. Tilt angles of transmembrane model peptides in oriented and non-oriented lipid bilayers as determined by 2H solid-state NMR. *Biophys. J.* 86:3709–3721.

32. MacKenzie, K. R., J. H. Prestegard, and D. M. Engelman. 1997. A *trans*membrane helix dimer: structure and implications. *Science*. 276:131–133.

33. Aisenbrey, C., P. Bertani, …, B. Bechinger. 2007. Structure, dynamics and topology of membrane polypeptides by oriented 2H solid-state NMR spectroscopy. *Eur. Biophys. J.* 36:451–460.

34. Lemmon, M. A., J. M. Flanagan, …, D. M. Engelman. 1992. Glycophorin A dimerization is driven by specific interactions between transmembrane α-helices. *J. Biol. Chem.* 267:7683–7689.

35. Shan, X., J. H. Davis, …, F. J. Sharom. 1994. 2H-NMR investigation of DMPC/glycophorin bilayers. *Biochim. Biophys. Acta.* 1193:127–137.

36. Wenk, M. R., T. Alt, …, J. Seelig. 1997. Octyl-β-D-glucopyranoside partitioning into lipid bilayers: thermodynamics of binding and structural changes of the bilayer. *Biophys. J.* 72:1719–1731.

37. Seelig, A. 1987. Local anesthetics and pressure: a comparison of dibucaine binding to lipid monolayers and bilayers. *Biochim. Biophys. Acta.* 899:196–204.

38. Beschiaschvili, G., and J. Seelig. 1992. Peptide binding to lipid bilayers. Nonclassical hydrophobic effect and membrane-induced pK shifts. *Biochemistry.* 31:10044–10053.

39. Phillips, M. C., R. M. Williams, and D. Chapman. 1969. On the nature of hydrocarbon chain motions in liquid crystals. *Chem. Phys. Lipids.* 3:234–244.

40. Seelig, J. 1981. Physical properties of model membranes and biological membranes. *In* Membranes and Intercellular Communication. R. Balian, M. Chabre, and P. F. Devaux, editors. North-Holland, Amsterdam. 15–78.

41. Heerklotz, H., and R. M. Epand. 2001. The enthalpy of acyl chain packing and the apparent water-accessible apolar surface area of phospholipids. *Biophys. J.* 80:271–279.

42. Wojtowicz, P. J. 1974. Introduction to the molecular theory of nematic liquid crystals. *In* Introduction to Liquid Crystals. E. B. Priestley, P. J. Wojtowicz, and P. Sheng, editors. Plenum Press, New York. 31–43.

43. Seelig, A., and J. Seelig. 1978. Lipid-protein interaction in reconstituted cytochrome *c* oxidase/phospholipid membranes. *Hoppe Seylers Z. Physiol. Chem.* 359:1747–1756.

44. Tamm, L. K., and J. Seelig. 1983. Lipid solvation of cytochrome *c* oxidase. Deuterium, nitrogen-14, and phosphorus-31 nuclear magnetic resonance studies on the phosphocholine head group and on *cis*-unsaturated fatty acyl chains. *Biochemistry.* 22:1474–1483.

45. Seelig, A., and J. Seelig. 1985. Phospholipid composition and organization of cytochrome *c* oxidase preparations as determined by 31P-nuclear magnetic resonance. *Biochim. Biophys. Acta.* 815:153–158.

46. Kobayashi, M., A. V. Struts, …, H. Akutsu. 2008. Fluid mechanical matching of H^+-ATP synthase subunit *c*-ring with lipid membranes revealed by 2H solid-state NMR. *Biophys. J.* 94:4339–4347.

47. Bloom, M., E. Evans, and O. G. Mouritsen. 1991. Physical properties of the fluid lipid-bilayer component of cell membranes: a perspective. *Q. Rev. Biophys.* 24:293–397.

48. Fisher, L. E., D. M. Engelman, and J. N. Sturgis. 2003. Effect of detergents on the association of the glycophorin A transmembrane helix. *Biophys. J.* 85:3097–3105.

49. Opatowski, E., M. M. Kozlov, …, D. Lichtenberg. 2002. Heat evolution of micelle formation, dependence of enthalpy, and heat capacity on the surfactant chain length and head group. *J. Colloid Interface Sci.* 246:380–386.

50. Opatowski, E., D. Lichtenberg, and M. M. Kozlov. 1997. The heat of transfer of lipid and surfactant from vesicles into micelles in mixtures of phospholipid and surfactant. *Biophys. J.* 73:1458–1467.

51. Capalbi, A., G. Gente, and C. La Mesa. 2004. Solution properties of alkyl glucosides, alkyl thioglucosides and alkyl maltosides. *Colloids Surf. A Physicochem. Eng. Asp.* 246:99–108.

52. Majhi, P. R., and A. Blume. 2001. Thermodynamic characterization of temperature-induced micellization and demicellization of detergents studied by differential scanning calorimetry. *Langmuir.* 17:3844–3851.